

The Co–Ni distribution in decagonal Al_{69.7(4)}Co_{10.0(4)}Ni_{20.3(4)}

Thomas Weber^{*I}, Björn Pedersen^{II}, Peter Gille^{III}, Friedrich Frey^{III} and Walter Steurer^I

^I Laboratory of Crystallography, Department of Materials, Wolfgang-Pauli-Strasse 10, 8093 Zurich, Switzerland

^{II} FRM II, TU München, 85747 Garching, Germany

^{III} Ludwig-Maximilians-Universität München, Department für Geo- u. Umweltwissenschaften, Sektion Kristallographie, Theresienstr. 41, 80333 München, Germany

Received June 18, 2008; accepted August 7, 2008

d-Al–Co–Ni / Charge-flipping / Low-density elimination / Neutron diffraction / Co–Ni ordering

Abstract. The Co–Ni distribution in *d*-Al_{69.7(4)}Co_{10.0(4)}Ni_{20.3(4)} was investigated based on X-ray and neutron diffraction data. The structure was modelled in higher dimensional space using the ‘charge-flipping’ and ‘low-density elimination’ methods and it was quantitatively refined in three-dimensional space employing a pseudo-approximant approach. In higher-dimensional description, the Co atoms are found at the centre of one of the two symmetry independent occupation domains, enclosed by regions mainly occupied by Ni. The other occupation domain is mostly occupied by Al. In physical space Co atoms are located in the centres of small Al pentagons and form pentagonal units, which are arranged in decagonal rings. On these sites Co is partly substituted by Ni, while all other transition metal sites are occupied by Ni and to a minor degree by Al. The fraction of Co found on transition metal sites decreases with decreasing Co–Co distances, whereby Co is replaced by Ni.

1. Introduction

Decagonal Al–Co–Ni certainly belongs to the best-characterized quasicrystalline systems (for a review see Steurer, 2004). Despite its fundamental importance for the understanding of crystal-chemical and physical properties, however, only little is known about the chemical ordering of Co and Ni on transition metal (TM) sites. This may be explained by the fact that the most common structure determination techniques, *i.e.* X-ray diffraction and electron microscopy, provide almost no contrast between Co and Ni. Atom location by channelling-enhanced microanalysis (‘ALCHEMI’) showed no indication for distinct chemical ordering of Co and Ni in samples of *d*-Al₇₂Ni₂₀Co₈ (Saitoh *et al.*, 2001) and *d*-Al₇₀Ni₁₈Co₁₂ (Saitoh *et al.*, 2004), though a minor degree of ordering could not be ruled out. Neutron diffraction experiments, on the other hand, allow distinguishing Co and Ni atoms (neutron scattering lengths:

$b_{\text{Al}} = 3.45$ fm, $b_{\text{Co}} = 2.50$ fm, $b_{\text{Ni}} = 10.30$ fm *vs.* X-ray atomic form factors: $f_{\text{Al}}(\mathbf{0}) = 13$, $f_{\text{Co}}(\mathbf{0}) = 27$, $f_{\text{Ni}}(\mathbf{0}) = 28$), but detailed investigations on TM ordering in the system *d*-Al–Co–Ni have so far not been performed. In this work we report the results of neutron and X-ray scattering experiments on the compound *d*-Al_{69.7(4)}Co_{10.0(4)}Ni_{20.3(4)}. Structure modelling was done by two complementary approaches. First, the structure was modelled in higher-dimensional (*n*D) space using charge-flipping (‘CF’, Oszlányi, Sütő, 2008) and low-density elimination (‘LDE’, Shiono, Woolfson, 1992, Takakura *et al.*, 2001a) methods. Since only little experience regarding qualitative and quantitative reliability of CF/LDE methods is available, we cross-checked the results by employing a 3D approach where the quasicrystal structure is transformed into a virtual approximant by appropriate shearing of the *n*D lattice. The obtained pseudo-approximant was refined quantitatively using conventional crystallographic tools.

2. Experimental and data reduction

Crystals were grown by the Czochralski method by slowly pulling (0.15 mm/h) from an incongruent melt of initial composition Al₇₇Co₆Ni₁₇ at a temperature of about 1050 °C. Use was made of [00001]-oriented native seeds that were prepared from a former crystal. The composition was analyzed from a sample taken from the neighbourhood of the crystals using a Cameca SX50 microprobe (15 kV, 10 nA). The experimental density of the sample was found to be 4190(2) kg/m³. The neutron diffraction experiment was done at the reactor FRM-II, Munich, Germany using the instrument RESI (Pedersen *et al.* 2006, Pedersen *et al.*, 2007) at a wavelength of 1.042 Å (Cu-422 monochromator, rotation images 0.5°, 1000 sec/image). This instrument is placed at the end of a neutron guide, providing very low background. It is equipped with a neutron sensitive image plate, providing a large coverage in reciprocal space, which is essential for quasicrystal work. The X-ray scattering experiment was done with an Oxford Diffraction diffractometer (‘Onyx’-CCD detector, Mo– K_{α} radiation, graphite monochromator). The diffraction pattern shows presence of S1 satellite reflections, but no S2 satellites (Fig. 1). The superstructure is not considered in

* Correspondence author (e-mail: thomas.weber@mat.ethz.ch)

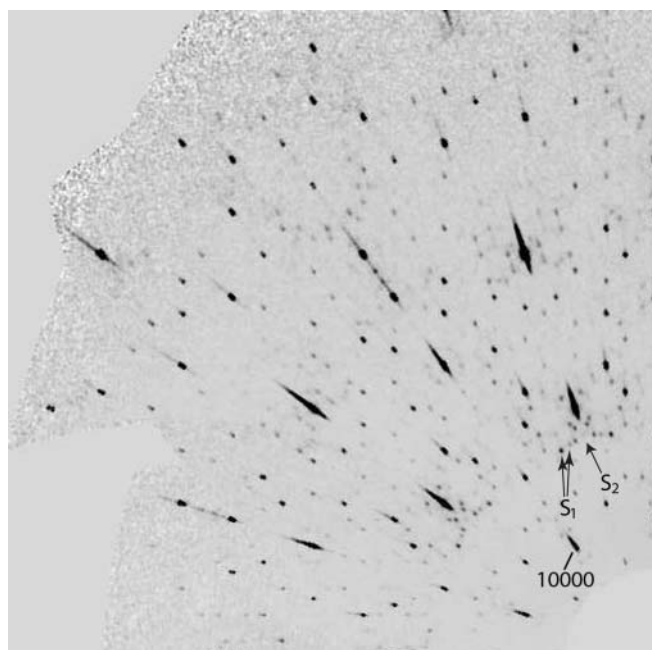


Fig. 1. X-ray diffraction pattern from the zeroth layer of $d\text{-Al}_{69.7(4)}\text{Co}_{10.0(4)}\text{Ni}_{20.3(4)}$. The 10000 reflection is indicated. The arrows show some positions of S_1 (present) and S_2 (absent) satellites.

the following, because the satellite intensities are very weak and the determination of superstructure ordering is beyond the scope of this work. Along the periodic direction weak diffuse interlayers are present indicating a disordered $\sim 8 \text{ \AA}$ superstructure. Main reflections could be indexed using a 5D decagonal lattice with $a_1^* \dots a_4^* = 0.2655(1) \text{ \AA}^{-1}$ and $a_5^* = 0.2448(2) \text{ \AA}^{-1}$ (lattice parameters taken from X-ray data). The definition of the basis is indicated by the 10000 reflection in Fig. 1. The number of reflections collected is 17735 (835 unique, $R_{\text{int}} = 3.6\%$) for X-rays and 548 (174 unique, $R_{\text{int}} = 4.8\%$) for neutrons.

3. Structure solution by charge flipping and low density elimination

CF and LDE are *ab-initio* Fourier recycling techniques, which provide phases of Bragg reflections in reciprocal space and scattering densities in real space. To enhance the comparability of X-ray and neutron scattering densities regarding truncation effects, only the 174 unique reflections present in both data sets were used. Further, experimental neutron intensities were multiplied by a squared, composition averaged X-ray atomic form factor, what has the effect that the neutron scattering based density peaks are broadened such that the atomic shapes are approximately the same as those obtained from X-ray experiments. According to the convolution theorem a multiplication in reciprocal space with a function $f(\mathbf{h})$ is accompanied by a convolution in real space with its Fourier transform $F(\mathbf{x})$. Therefore, this manipulation has no effect on the relative atomic scattering power obtained from the neutron data, *i.e.* it is proportional to the neutron scattering length and not to the number of electrons of the respective atoms. Using normalised X-ray intensities by

dividing the X-ray data by a squared, composition averaged atomic form factor, would also yield comparable X-ray/neutron scattering density maps, now showing sharpened atoms in the X-ray case. A disadvantage of this approach is that the influence of systematic and statistical errors of weak X-ray intensities is enhanced and truncation effects become more dominant in the scattering density maps. The latter would hamper the performance of CF/LDE optimizations, as both techniques rely on the assumption of positive scattering densities (for a proper handling of negative scattering lengths in neutron diffraction experiments see Oszlányi, Sütő, 2007). Structure determination was done in 5D space using the program SUPERFLIP (Palatinus *et al.*, 2007). The experimental data were expanded to a full sphere according to the observed Laue symmetry $10/mmm$, but the structure refinement was done without any symmetry constraint in the 5D space group P1. To reduce statistical noise, LDE and CF optimizations were repeated 100 times to full convergence with different random number generator seeds. The resulting patterns were averaged after shifting the scattering densities to a same origin. In all cases CF and LDE converged without problems within less than 100 cycles. CF and LDE refinements gave essentially the same results, however, scattering densities obtained by CF appeared to be slightly noisier than LDE results. Finally, a common scale factor was determined by minimizing the difference between X-ray and neutron density maps.

Within a 5D unit cell four occupation domains (ODs) are found from which two are symmetry independent (OD1 at $1/5 \ 1/5 \ 1/5 \ 1/5 \ 1/4$ and $4/5 \ 4/5 \ 4/5 \ 4/5 \ 3/4$, OD2 at $2/5 \ 2/5 \ 2/5 \ 3/4$ and $3/5 \ 3/5 \ 3/5 \ 3/5 \ 1/4$; see Fig. 2). All ODs show $5m$ eigen-symmetry in good approximation. The ODs obtained from neutron and X-ray data are very similar: in both cases OD2 shows a stronger average density than OD1 (Fig. 2). As the scattering densities are not symmetry averaged, some weak and featureless deviations from a perfect $5m$ symmetry are visible. According to the relative strength of scattering factors in neutron and X-ray experiments, the following qualitative scheme may be used for identification of elements: Ni is present in the regions, where scattering densities are strong in both cases, Al is related to weak X-ray and neutron scattering densities, while Co is indicated by scattering densities, which are weak in the neutron and strong in the X-ray case. The presence of mixed positions and truncation effects, however, do not allow definite conclusions. A much clearer picture about the Co distribution is expected to be found in the difference between neutron and X-ray density patterns. Ni and Al have roughly a same relative scattering power in X-ray and neutron case, *i.e.* in a difference map they are expected to show a small contrast, while Co diffracts much weaker in neutron experiments and is supposed to provide a strong contrast.

In Fig. 2 it is seen that a strong negative peak is present at the centre of OD2 when subtracting X-ray from neutron densities. There is no significant difference density for OD1, *i.e.* Co atoms are exclusively located in the centre of OD2. The outer part of OD2 is dominated by strong densities for both, X-ray and neutron data. Therefore, this part is mainly occupied by Ni atoms, while Al

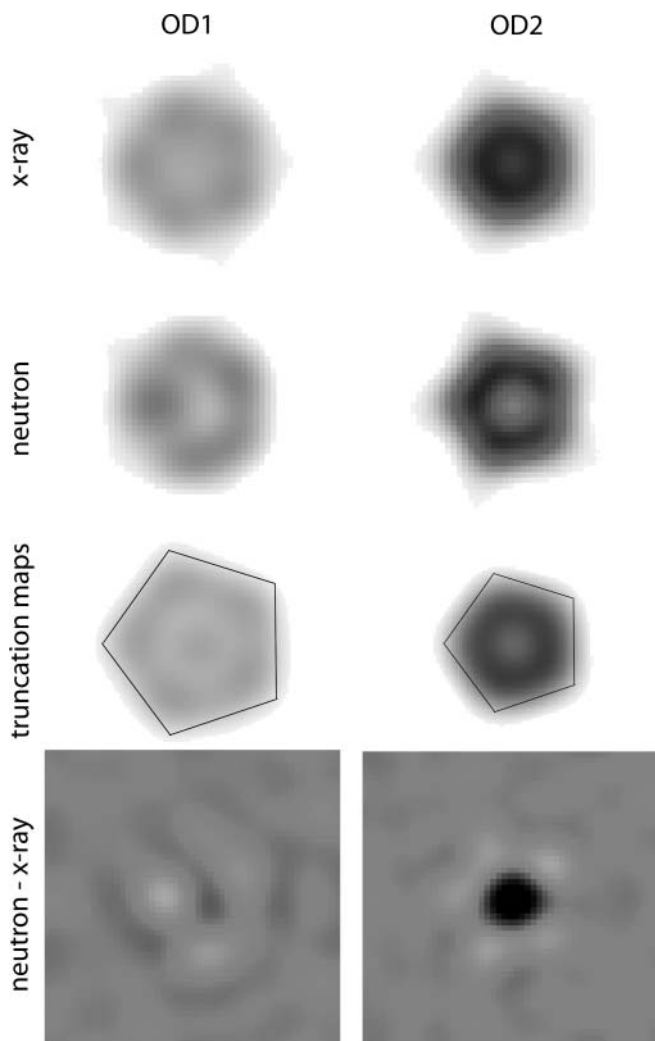


Fig. 2. Perpendicular space sections of OD2 and OD1 as obtained from LDE modelling. X-ray, neutron and difference scattering density maps are shown, as well as a map for estimating truncation effects (see text). The pentagons show the size of the respective ODs used for the calculation of the truncation maps. The grey background in the difference maps indicate the zero level; at darker regions X-ray densities are higher than neutron densities and *vice versa*.

atoms are predominately found in OD1, which has weak densities in both cases. A minor contribution of Ni to the outer part of OD1, as found by Takakura *et al.* (2001*b*) for a quasicrystal with similar composition ($d\text{-Al}_{72}\text{Ni}_{20}\text{Co}_8$) cannot be excluded. It is noticeable that all ODs show minima at the centre, even in the X-ray case, where high densities are expected due to the presence of Co. This behaviour may be explained by truncation effects as a consequence of the very limited experimental data sets. In Fig. 2, estimates for the errors introduced by truncation effects are given. The truncation maps were obtained from a simplified model where idealized pentagonal ODs of estimated size were fully occupied by Al (OD1) or TMs (OD2). From this model, X-ray Bragg intensities were calculated for the same set of 174 Bragg reflections used for analyzing the experimental structure and the structure was re-determined using LDE as described above. Since truncation effects are sensitive to details of the structure, a perfect description cannot be obtained (in particular, the truncation map of OD1 shows a small maximum in the



Fig. 3. $75 \text{ \AA} \times 75 \text{ \AA}$ sized X-ray, neutron and difference scattering density maps as obtained by LDE. The Co atom positions are clearly identified in the difference map (dark difference densities have a higher density in the X-ray than in the neutron case, the gray background indicates the zero level). As indicated, Co atoms arrange in pentagonal units, which form decagonal rings. Dashed and solid line motifs are related by a scale factor τ .

centre that is not present in the experimental OD1), but it is clearly seen that the broad depressions at the centres of the ODs may be explained by the limited set of diffraction data. Nevertheless, mixed Co/Al occupancies or vacancies at Co positions cannot be completely ruled out from these results (see, however, below).

Figure 3 shows $75 \text{ \AA} \times 75 \text{ \AA}$ physical space sections of the structure as obtained by LDE. Again the Co positions can be clearly identified in the difference maps. They are found in the centres of small, partly disordered pentagons, which in the X-ray as well as in the neutron case consist of low scattering density atoms, *i.e.* they are built of Al. As seen in Fig. 3c, the Co atoms are arranged in pentagonal units forming decagonal rings. Positions connected by solid lines are strongly occupied by Co. In a $1/\tau$ scaled ring (dashed lines) Co still occupies the vertices of pentagons, but now the vertices of the decagons become closer and less occupied by Co. If further scaled by $1/\tau$ (not marked in Fig. 3), the vertices of the pentagons become practically fully occupied by Ni. It can therefore be concluded that the probability of finding Co on TM sites decreases the shorter Co–Co distances are. Co is replaced by Ni as the total concentration of TMs on corresponding sites seems to be unaffected by the variation of Co (*cf.* Figs. 3a and c). Other Ni sites are found in pentagonal units enclosed in the Co pentagons. The Ni pentagons are rotated by 36° and scaled by $1/\tau^2$ relative to the hosting Co pentagons.

4. Pseudo-approximant approach

As demonstrated by Katrych *et al.* (2007), transformation of quasicrystal Bragg indices to a 3D pseudo-approximant lattice allows a quick and easy to use approach to local structure motifs, if details about the global structure ordering are not of interest. The transformation can be understood as a shear of the nD lattice such that the physical space cut has a rational slope relative to the 5D hyperlattice. The resulting periodic approximant structure does not (necessarily) exist in reality, but provides a reasonable representation of structure motifs in the quasicrystal that are smaller than the pseudo-approximant unit cell. In general, it is expected that the agreement between the pseudo-approximant and the real quasicrystal increases with a decreasing size of the motifs. The pseudo-approximant approach is therefore a robust test for the results described in the previous chapter.

The quasicrystal diffraction data were transformed to a $3/5$ approximant lattice as described by Katrych *et al.* (2007). The lattice obtained is orthorhombic with $a = 31.783 \text{ \AA}$, $b = 23.092 \text{ \AA}$ and $c = 4.083 \text{ \AA}$. The structure was refined in space group $Cmcm$. The sub-group $C2cm$ was also tested, but no significant improvement of the fit was found. The pseudo-approximant structure was solved with the program SUPERFLIP, and a joint refinement against X-ray and neutron data was done with the program package JANA2006 (Petricek *et al.*, 2006). Contrary to CF/LDE runs all available diffraction data were used in the least squares refinement. The refinement converged to an overall R -value of 13.9% ($R_{X\text{-ray}} = 13.1\%$, $R_{\text{neutr}} = 14.5\%$) for observed reflections with $I > 3\sigma$.

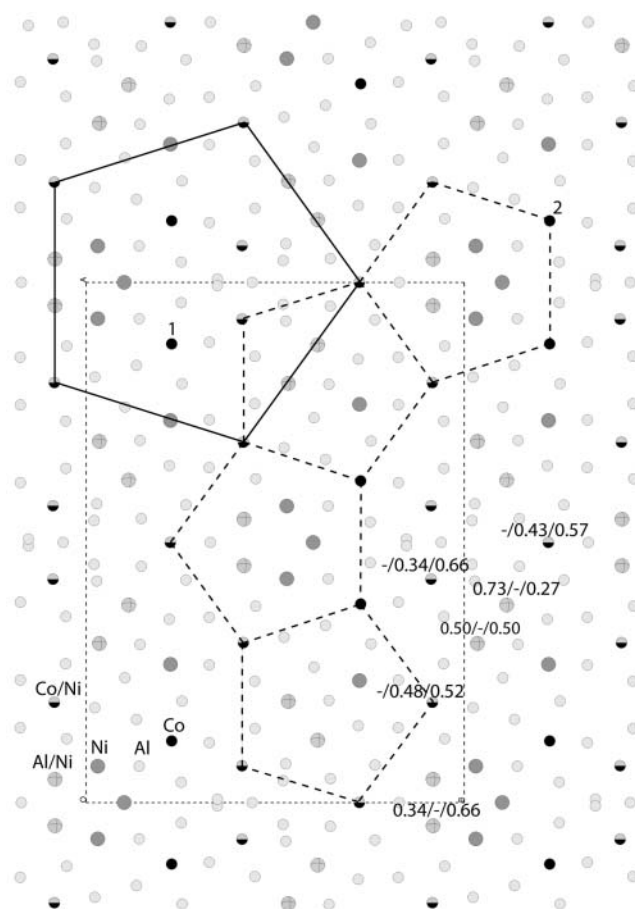


Fig. 4. Section of the pseudo-approximant structure. The occupancies of mixed positions are shown by the scheme $occ(\text{Al})/occ(\text{Co})/occ(\text{Ni})$. All other positions are fully occupied by one element except for split positions, which respective sums give a full occupancy. Atoms labelled '1' and '2' are examples for symmetry equivalent atoms in the approximant structure, which in the quasicrystal case are different from a crystal-chemical point of view. The pentagons mark motifs built by Co that are also found in the quasicrystal (*cf.* Fig. 3).

Although not perfect, the calculated density (4352 kg/m^3) as well as the refined composition ($\text{Al}_{70.7}\text{Co}_{8.3}\text{Ni}_{21.0}$) are in a good agreement with the experimental results. Small deviations from the experimental values may be explained by errors introduced by the transformation of the quasicrystalline lattice to a periodic pseudo-approximant, which cannot yield a perfect representation of the quasicrystal. The lower experimental density may further be explained by the presence of pores in the sample, which are frequently observed in quasicrystals. The resulting structure is seen in Fig. 4. As indicated by the pentagons, major structure motifs found by CF/LDE are reproduced in the periodic structure in good approximation and therefore nicely confirm the conclusions drawn above. There are some minor discrepancies between the results from the CF/LDE and from pseudo-approximant approaches. In particular, the relative site occupancies of Co show deviations and some sites occupied by Co in the periodic structure are not occupied by Co in the quasicrystal maps (*e.g.* the atom labelled by '1' in Fig. 4). This behaviour may be explained by the periodic symmetry artificially superimposed to the structure. If, for example, atom '2' in Fig. 4 is occupied by Co, then atom '1' must also be occupied

by Co due to *Cmcm* symmetry, even if not expected from a chemical point of view. It was further tested, whether sites mixed occupied by Al/Ni and Co/Ni may host Co or Al/voids, respectively, but no significant contributions could be found. This is a further indication that the minima observed in the centres of OD2 seen in Fig. 2 are coming from truncation effects and not from Co/Al or Co/void substitutions.

5. Conclusions

In summary, it has been experimentally proven that Co and Ni show at least partial chemical ordering in the compound under investigation. In superspace, transition metals exclusively occupy one of the two occupation domains, whereby Co/Ni is found close to the centre and Ni/Al at the outer part. The second occupation domain is probably completely filled by Al, but a small fraction of Ni would be consistent with our results. In three-dimensional space Co atoms exclusively occupy centres of small pentagonal rings built of Al, where they are partly substituted by Ni if Co–Co distances become short. Co atoms are arranged in pentagonal units, which form decagonal rings. On the other hand, Ni is mainly found in smaller pentagonal units, which are rotated by 36° and scaled by $1/\tau^2$ relative to the hosting Co pentagons. This allows the conclusion that short Ni–Ni distances are by far more favourable than short Co–Co distances. At such positions, Ni is not substituted by Co, but to a minor degree by Al. The results of this work are in a good agreement with theoretical calculations, where it was concluded that the most favourable next neighbour interactions in *d*-Al–Co–Ni are Co–Al, Ni–Ni and Ni–Al (Mihalkovic *et al.*, 2002, Henley *et al.*, 2002), *i.e.* Co prefers Al coordination. It can further be concluded that CF/LDE as well as the pseudo-approximant approach give consistent and reasonable results and are well suited for qualitative and semi-quantitative studies of building principles in quasicrystals.

References

- Henley, C. L.; Mihalkovic, M.; Widom, M.: Total-energy-based structure prediction for d(AlNiCo). *J. Alloys Compd.* **342** (2002) 221–227.
- Katrych, S.; Weber, T.; Kobas, M.; Massüger, L.; Palatinus, L.; Chapuis, G.; Steurer, W.: New stable quasicrystal in the system Al–Ir–Os. *J. Alloys Compd.* **428** (2007) 164–172.
- Mihalkovic, M.; Al-Lehyani, I.; Cockayne, E.; Henley, C.L.; Moghadam, N.; Moriarty, J. A.; Wang, Y.; Widom, M.: Total-energy-based prediction of a quasicrystal structure. *Phys. Rev.* **B65** (2002), art. no.-104205.
- Oszlányi G.; Sütő, A.: Ab initio neutron crystallography by the charge flipping method. *Acta Crystallogr.* **A63** (2007) 156–163.
- Oszlányi G.; Sütő, A.: The charge flipping algorithm. *Acta Crystallogr.* **A64** (2008) 123–134.
- Palatinus, L.; Chapuis, G.: SUPERFLIP – a computer program for the solution of crystal structures by charge flipping in arbitrary dimensions. *J. Appl. Cryst.* **40** (2007) 786–790.
- Pedersen B.; Frey F.; Scherer W.; Gille P.; Meisterernst G.: The new single crystal diffractometer RESI at FRM-II. *Physica B* **385–386** (2006) 1046–1048.
- Pedersen, B.; Frey, F.; Scherer, W.: The single crystal diffractometer RESI. *Neutr. News* **18** (2007) 20–22.
- Petricek, V.; Dusek, M.; Palatinus, L.: Jana2006. The crystallographic computing system. (2006) Institute of Physics, Praha, Czech Republic.
- Saitoh, K.; Tanaka, M.; Tsai, A. P.; Rossouw, C.J.: ALCHEMI study of an Al₇₂Ni₂₀Co₈ decagonal quasicrystal. *Ferroelectr.* **250** (2001) 207–212.
- Saitoh, K.; Tanaka, M.; Tsai, A. P.: ALCHEMI study of an S1-type superlattice-ordered decagonal quasicrystal of Al₇₀Ni₁₈Co₁₂. *J. Non-Cryst. Solids* **334–335** (2004) 202–206.
- Shiono, M.; Woolfson, M. M.: Direct-space methods in phase extension and phase determination. I. Low-density elimination. *Acta Crystallogr.* **A48** (1992) 451–456.
- Steurer, W.: Twenty years of structure research on quasicrystals. Part 1. Pentagonal, octagonal, decagonal and dodecagonal quasicrystals. *Z. Kristallogr.* **219** (2004) 391–446.
- Takakura, H.; Shiono, M.; Sato, T. J.; Yamamoto, A.; Tsai, A. P.: Ab initio structure determination of icosahedral Zn–Mg–Ho quasicrystals by density modification method. *Phys. Rev. Lett.* **86** (2001a) 236–239.
- Takakura, H.; Yamamoto, A.; Tsai, A.P.: The structure of a decagonal Al₇₂Ni₂₀Co₈ quasicrystal. *Acta Crystallogr.* **A57** (2001b) 576–585.